Integrating Acousto-Optic Channelized Receivers

PETER KELLMAN, MEMBER, IEEE, HARRY N. SHAVER, MEMBER, IEEE, AND J. WILLIAM MURRAY, MEMBER, IEEE

Abstract—**The subject of this paper is acousto-optic channelized receivers with large noncoherent processing gain. A receiver model is developed and the output statistics are derived for signal plus noise input. Noise equivalent bandwidths and signal detection sensitivity are calculated. The implications of large average noise power are discussed. Experimental measurements are in agreement with the theory presented.**

I. Introduction

ACOUSTO-OPTIC (AO) techniques for power spectral measurement have been exploited for a variety of signal analysis applications [1]. Application of AO techniques to integrating channelized receivers with large noncoherent processing gain is the subject of this paper. Particular emphasis is given to detection of signals buried in noise. The key attributes of AO technology for this application are wide instantaneous bandwidth, a large number of spectral samples, and high-detection sensitivity.

The AO channelized receiver realizes high sensitivity and multiple-signal handling ability by means of channelization. Increased sensitivity may be achieved through noncoherent integration [2]. Special attention to receiver noise loading, system stability, and linearity is required to achieve significant processing gain. A receiver model is developed and the output mean and variance are calculated for signal plus noise input. The treatment in this paper relates the noise equivalent channel bandwidth to optical parameters. The degradation in signal detection sensitivity due to noise arising in the photodetection process is derived. It is shown that a tradeoff between noncoherent processing gain and output dynamic range exists due to the increase in average noise power bias with increasing integration. Implications of average noise power loading to receiver design are discussed. Receiver processor considerations such as digital quantization noise and threshold settability are included. Experimental noise measurements are in agreement with the theory presented.

II. Acousto-Optic Channelized Receiver Model

A conceptual diagram of the AO channelized receiver is shown in Fig. 1. A first-order theory of operation is reviewed. A transparent ultrasonic delay line (Bragg cell) is utilized to convert a wide-band electrical input to a proportional optical pattern by means of a traveling pressure wave. Spatial variation created in the refractive index is used to modulate coherent light, and the diffracted spectral components are separated by a lens. The Fourier transform of the input signal results as a light distribution in the focal plane of the lens. This light distribution is detected photoelectronically, producing a charge distribution proportional to the instantaneous power spectrum of the input signal. Integrated charge packets at discrete photosites are then multiplexed to produce a sampled data waveform.

An expression for the detected output voltage samples is now derived in terms of the input signal $u(t)$. The sliding window power spectrum at time t can be written as

$$\left| \int_{-\infty}^{\infty} w(\tau)\, u(t-\tau) \exp(-i2\pi f\tau)\, d\tau \right|^2$$

where the window function $w(t)$ determines the spectral resolution. The complex window function $w(t)$ represents both amplitude and phase factors. Contributions to the amplitude window function include the finite delay length, uniformity of illumination, acoustic attenuation, and diffraction. Phase contributions include lens aberrations, optical surface inaccuracies, and focusing errors.

Utilizing a discrete array of photodetectors gives rise to a sample spectrum

$$\int_{-\infty}^{\infty} H(f-f_k) \left| \int_{-\infty}^{\infty} w(\tau)\, u(t-\tau) \exp(-i2\pi f\tau)\, d\tau \right|^2 df$$

where f_k is the frequency corresponding to the kth detector and $H(f)$ is a spectral weighting function that describes the spatial response of an individual detector element. This weighting function includes the contribution of electrical crosstalk between channels that may occur in the readout process. In particular, the inefficiency of charge transfer devices broadens the spectral weighting. Variation between array elements has been neglected.

The instantaneous power spectrum is integrated in time producing a voltage

$$X_{jk} = \int_{jT}^{(j+1)T} \int_{-\infty}^{\infty} H(f-f_k) \cdot \left| \int_{-\infty}^{\infty} w(\tau)\, u(t-\tau) \exp(-i2\pi f\tau)\, d\tau \right|^2 df\, dt \quad (1)$$

where j denotes the sample time and T equals the integration period.

The output sampled data value

$$Z_{jk} = X_{jk} + Y_{jk} \quad (2)$$

includes an additive detection noise contribution Y_{jk}. Detection noise has both thermal and shot components. Shot noise depends on the average optical power and is therefore signal

Manuscript received August 22, 1980.
The authors are with the ESL Incorporated, 495 Java Drive, P.O. Box 510, Sunnyvale, CA 94086.

0018-9219/81/0100-0093$00.75 © 1981 IEEE

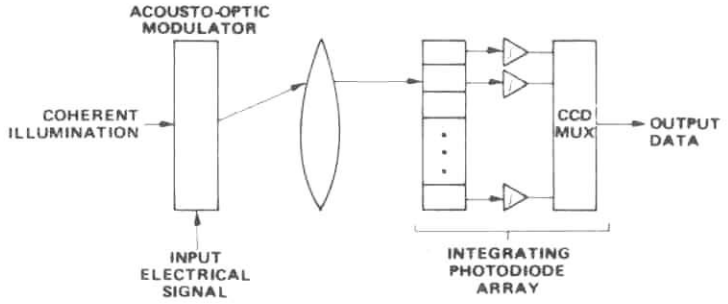

Fig. 1. AO channelized receiver concept.

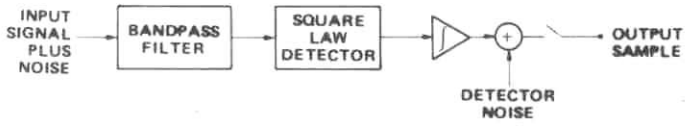

Fig. 2. Simplified channel model.

dependent. Thermal noise, due to random agitation of electrons and reset charge uncertainty, is independent of the optical signal. The relative importance of thermal versus shot noise depends on the number of photo electrons. It will be shown that shot noise effects are negligible for devices with more than several hundred rms thermal noise electrons.

A simplified model of a single receiver channel is shown in Fig. 2. This model is useful in first order calculations of receiver sensitivity and noise figure. However, it will be shown this simple channel model is not precise since it does not include the effect of a spectral weighting function $H(f)$.

III. Noise Equivalent Bandwidth

The output detection statistics are calculated based on the receiver model described in the previous section, equations (1) and (2). Detailed derivation is lengthy, therefore, only important results are stated in the text (derivations are outlined in Appendix A). Signal-to-noise ratios are defined and noise equivalent bandwidths are derived. The noise equivalent bandwidth is expressed in terms of the input window and spectral weighting functions. The equivalent bandwidth is signal dependent due to spectral averaging. Two cases are analyzed: sinusoid plus noise and random signal plus noise.

Consider a signal plus noise input

$$u(t) = s(t) + n(t) \tag{3}$$

where $n(t)$ is zero mean white Gaussian noise with noise power spectral density $N_0/2$ (i.e., the noise autocorrelation is

$$R_n(\tau) = E\{n(t)\, n(t-\tau)\} = (N_0/2)\delta(\tau)).$$

The mean output,

$$\mu_Z = E\{Z_{jk} = X_{jk} + Y_{jk}\} = E\{X_{jk}\} = \mu_X = \mu_s + \mu_n \tag{4}$$

is the sum of the mean output signal power μ_s and the mean output noise power μ_n. It may be shown that μ_n is given by

$$\mu_n = \frac{N_0 T}{2} \int G(f)\, df \int H(f')\, df' \tag{5}$$

where $G(f)$ is the magnitude squared of the Fourier transformed window function,

$$G(f) = \left| \int w(\tau) \exp(-i2\pi f\tau)\, d\tau \right|^2. \tag{6}$$

The output noise variance σ_Z^2 is given by

$$\sigma_Z^2 = \sigma_X^2 + \sigma_Y^2. \tag{7}$$

The detector noise variance σ_Y^2 degrades the output signal-to-noise ratio. Detection sensitivity loss is examined in the following section.

For a sinusoidal input,

$$s(t) = A \cos[2\pi f_0 t + \phi] \tag{8}$$

the mean output signal power can be written as

$$\mu_s = \frac{A^2 T}{4} \mathcal{H}(f_k - f_0) \tag{9}$$

where $\mathcal{H}(f)$ is the convolution between the functions G and H,

$$\mathcal{H}(f) = \int G(f - f')\, H(f')\, df'. \tag{10}$$

The variance for a sinusoid plus noise input $\sigma_{X_{s+n}}^2$ can be expressed in terms of the variance for noise only input $\sigma_{X_n}^2$ in the familiar form

$$\sigma_{X_{s+n}}^2 = \sigma_{X_n}^2 (1 + 2\,\mathrm{SNR}_i) \tag{11}$$

where

$$\sigma_{X_n}^2 = \left(\frac{N_0}{2}\right)^2 T \int \mathcal{H}^2(f)\, df \tag{12}$$

and the input signal-to-noise ratio $\mathrm{SNR}_i = A^2/2B_sN$ is measured in the noise equivalent bandwidth B_s. The noise equivalent bandwidth B_s for the case of sinusoid plus noise input, equals

$$B_s = \frac{\int \mathcal{H}^2(f)\, df}{\mathcal{H}^2(0)}. \tag{13}$$

The signal-to-noise ratio of the variable X_{jk} can be defined as

$$\mathrm{SNR}_X = \mu_s^2/\sigma_{X_n}^2 \tag{14}$$

where the mean noise power μ_n has been subtracted. The output signal-to-noise ratio SNR_X can be related to the input signal-to-noise ratio SNR_i as

$$\mathrm{SNR}_X = B_s T\, \mathrm{SNR}_i^2. \tag{15}$$

It has been assumed that the input frequency $f_0 = f_k$. An alternative definition for output signal-to-noise ratio uses the signal plus noise variance, yielding

$$\frac{\mu_s^2}{\sigma_{X_{s+n}}^2} = B_s T \frac{\mathrm{SNR}_i^2}{1 + 2\,\mathrm{SNR}_i} \tag{16}$$

which is approximately the same as (15) for low input signal-to-noise ratio. The latter definition exhibits linear behavior for a sinusoid input at high signal-to-noise ratio.

The processing gain may be defined as the ratio of the input signal-to-noise ratio without integration, to the input signal-to-noise ratio with integration in order to achieve the same detection probability. The processing gain is proportional to $\sqrt{B_s T}$.

The above formulation for sinusoid plus noise input is approximately valid for signals with narrow-band modulation. However, as the modulation bandwidth approaches the channel bandwidth, the signal spectrum interacts with the spectral weighting and thereby alters the effective time–bandwidth product.

Consider the case of a random Gaussian input signal $s(t)$ with uniform spectral density $S/2$, independent of the additive noise $n(t)$. The input signal-to-noise ratio in an arbitrary bandwidth is $\mathrm{SNR}_i = S/N_0$. It can be shown that the mean and variance are

$$\mu_X = \mu_n (1 + \mathrm{SNR}_i) \tag{17}$$

and

$$\sigma_{X_{s+n}}^2 = \sigma_{X_n}^2 (1 + \mathrm{SNR}_i)^2. \tag{18}$$

The signal-to-noise ratio defined by Equation (14) becomes

$$\mathrm{SNR}_X = \frac{\mu_n^2}{\sigma_{X_n}^2} \mathrm{SNR}_i^2 = B_n T\, \mathrm{SNR}_i^2 \tag{19}$$

where the noise equivalent bandwidth B_n is given by

$$B_n = \frac{\left[\int G(f)\,df \int H(f)\,df\right]^2}{\int \mathcal{H}^2(f)\,df}. \tag{20}$$

Using the alternative definition of signal-to-noise ratio (16), we have

$$\frac{\mu_s^2}{\sigma_{X_{s+n}}^2} = B_n T \frac{\mathrm{SNR}_i^2}{(1 + \mathrm{SNR}_i)^2}. \tag{21}$$

By this definition, the output signal-to-noise ratio never exceeds $B_n T$ for the case of random noise input.

Noise equivalent bandwidths have been derived for sinusoidal and wideband random input signals. The discrepancy between noise equivalent bandwidths B_s and B_n is due to averaging the spectral power. It can be shown that B_s is less than or equal to B_n. For Gaussian functions $G(f)$ and $H(f)$ the ratio B_n/B_s equals 2.

The probability of detection and false alarm depend on the probability distribution of the detection statistic. The distribution of the variable Z_{jk} is approximately Gaussian for large time–bandwidth product. In the preceding calculations, it has been assumed that the time–bandwidth product is much greater than one. Probability densities for noise only and signal plus noise inputs are illustrated in Fig. 3. This figure illustrates the relatively large mean noise level μ_n with respect

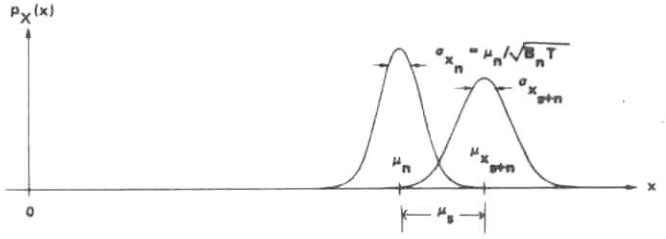

Fig. 3. Representative probability densities.

to the standard deviation σ_{X_n} that occurs as a consequence of integration. Receiver operating characteristics, i.e., probability of detection versus probability of false alarm, are easily calculated for Gaussian statistics.

IV. Receiver Noise Loading

The mean noise power level relative to the standard deviation increases with integration resulting in a bias. The presence of bias results in a tradeoff between receiver sensitivity and dynamic range. Evaluation of signal-to-noise ratio loss due to detection noise and the effect of average noise power loading are quantified below.

Receiver noise figures are typically determined by the receiver front end, since subsequent stages are preceded by sufficient gain in order to overcome additional noise. The integrating AO channelized receiver may likewise be operated with sufficient gain to overcome photodetection noise, provided that the mean noise level is tolerable.

Define the relationship between receiver noise σ_{X_n} and detection noise σ_Y as

$$\sigma_{X_n} = K\sigma_Y. \tag{22}$$

At this noise setting the mean noise level becomes

$$\mu_n = \sqrt{B_n T}\,\sigma_{X_n} = K\sqrt{B_n T}\,\sigma_Y. \tag{23}$$

If the detector dynamic range DR is defined as the maximum signal divided by the rms detector noise without input noise loading (i.e., $DR = Z_{\max}/\sigma_Y$), then the receiver dynamic range with noise loading $\widetilde{DR} = (Z_{\max} - \mu_n)/\sigma_Z$ can be expressed as

$$\widetilde{DR} = \frac{DR}{\sqrt{1 + K^2}} - \sqrt{\frac{K^2}{1 + K^2} B_n T}. \tag{24}$$

Equation (24) defines a tradeoff between dynamic range and processing gain $\sqrt{B_n T}$ for a fixed value of K. A further consideration is that the shot noise component becomes more significant with increasing mean noise level. Shot noise effects are treated in Appendix B.

The output signal-to-noise ratio degradation due to detector noise can be expressed through the ratio

$$\rho^2 = \frac{\mathrm{SNR}_X}{\mathrm{SNR}_Z} = 1 + \left(\frac{\sigma_Y}{\sigma_{X_n}}\right)^2 \tag{25}$$

where $\mathrm{SNR}_Z = \mu_s^2/\sigma_Z^2$. The input sensitivity loss ρ equals,

$$\rho = \sqrt{\frac{1 + K^2}{K^2}}. \tag{26}$$

The receiver dynamic range can be written in terms of ρ as

$$\widetilde{DR} = \sqrt{\frac{\rho^2 - 1}{\rho^2}}\, DR - \frac{1}{\rho}\sqrt{B_n T}. \tag{27}$$

Equations (26) and (27) are plotted in Figs. 4 and 5. Fig. 4 illustrates the large sensitivity loss that occurs as the detector noise exceeds the noise contribution due to the input. In Fig. 5 the detector dynamic range value is assumed to be $DR = 1000$ peak/rms (30 dB). For example, with $B_n = 1$ MHz, $T = 10$ ms, $DR = 1000$, and $\rho = 1.26$ (1 dB); the receiver dynamic range equals $\widetilde{DR} = 529$ (27.2 dB), therefore, noise loading has reduced the effective dynamic range by 2.8 dB.

The presence of a mean noise power output resulting from noncoherent integration places stringent requirements on system linearity and gain stability in order to realize the expected improvement in detection sensitivity. Susceptibility to gain variation depends to a large extent on the specific detection algorithm.

The effect of gain uncertainty is illustrated for the simplest detection scheme, a fixed threshold. The threshold must detect differences between the mean noise μ_n and signal plus noise $\mu_n + \mu_s$. If the gain changes by the fraction $(\Delta G/G)$, then the output signal level for a noise only input signal will be biased by $(\Delta G/G)\sqrt{B_n T}$ standard deviations. To maintain a probability of false alarm (P_{fa}) that does not exceed a specified value, the threshold level must necessarily be set for the condition where the gain is at (or greater than) its maximum value $G_{\max}$. If the gain decreases then the input signal power required to provide a specified probability of detection (P_d) increases. The maximum loss in receiver sensitivity occurs when the gain changes to its minimum value $G_{\min}$. For sinusoid plus noise input this can be computed from the relation

$$\max\{\text{loss}\} = 1 + Q + \left[1 - \sqrt{\frac{\text{TNR}_X}{\text{SNR}_X}}\right]\left[\sqrt{1 + 2Q\sqrt{\frac{\text{SNR}_X}{B_s T}}} - 1\right] \tag{28}$$

where

$$Q = \frac{\Delta G}{G_{\min}}\sqrt{\frac{B_n T}{\text{SNR}_X}}\left[1 + \sqrt{\frac{\text{TNR}_X}{B_n T}}\right]$$

$$\Delta G = G_{\max} - G_{\min}$$

$$\sqrt{\text{TNR}_X} = \frac{1}{\sigma_{X_n}}[(\text{Threshold Level}\,|\,P_{fa}) - \mu_n].$$

For example, with $B_n T = 10000$, and P_d, P_{fa} corresponding to an output signal-to-noise ratio of 10 dB, a decrease in gain of 1 dB will reduce the input sensitivity approximately 10 dB. Techniques such as noise riding thresholds and Dicke switching have been exploited to overcome gain sensitivity [3]. However, these approaches generally suffer operational restrictions, reduced sensitivity, and increased complexity.

V. Digital Processing

The ability to set precise thresholds and to estimate the noise statistics is required for signal detection. The functions of signal detection and accurate receiver calibration can be implemented through digital processing of the channelized receiver data. Further sensitivity improvement and increased dynamic range may be realized by digital integration with extended precision.

Define the digitized receiver output as

$$\hat{Z}_{jk} = Z_{jk} - \epsilon_{jk} \tag{29}$$

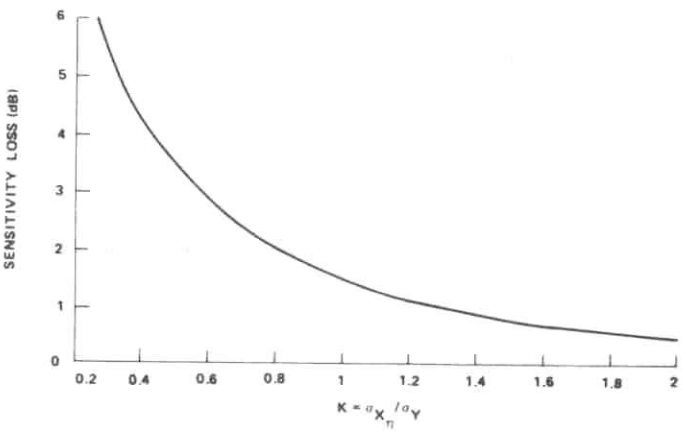

Fig. 4. Sensitivity loss versus receiver noise loading.

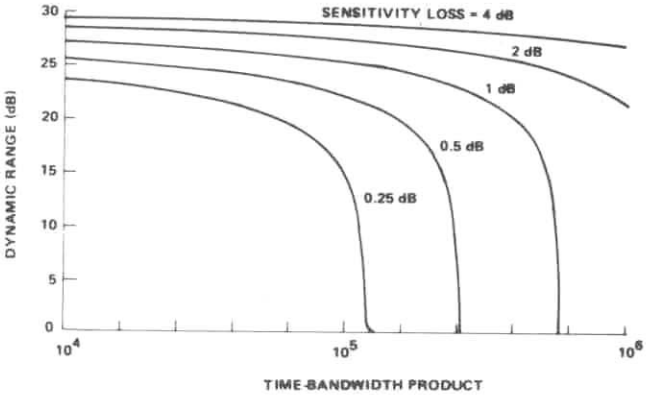

Fig. 5. Dynamic range versus time-bandwith product.

where ϵ_{jk} is the quantization error. The quantization error may be modeled [4] as zero mean independent noise, uniformly distributed with variance $\sigma_q^2 = q^2/12$, where q is the quantization step size. The assumption that the quantization error is independent of the signal is valid provided that the rms noise σ_{X_n} is comparable with the quantization step size q. The digital data has mean μ_X and variance

$$\sigma_{\hat{Z}}^2 = \sigma_X^2 + \sigma_Y^2 + \sigma_q^2. \tag{30}$$

In a manner similar to the development in Section IV, define the relationship between receiver noise standard deviation and detection plus quantization noise as

$$\sigma_{X_n} = K'\sqrt{\sigma_Y^2 + \sigma_q^2}. \tag{31}$$

The loss in sensitivity is then given by equation (26) and the dynamic range by equation (27) with the quantity K' replacing K. With this modification the curves of Figs. 4 and 5 apply to the digitized signal.

Digital integration improves the receiver sensitivity and increases the dynamic range. The mean noise spectrum estimate is improved and the precision of threshold settability increases with digital integration. However, additional bits must be maintained in the accumulation process in order to derive these benefits. Linear analog-to-digital conversion is used in order to subtract the mean noise spectrum prior to nonlinear distortion.

The digital integrated data can be written as,

$$V_{mk} = \sum_{j=mJ}^{(m+1)J} \hat{Z}_{jk} \tag{32}$$

where J is the number of samples integrated. The mean and variance are given as

$$\mu_V = J\mu_X \tag{33}$$

and

$$\sigma_V^2 = J\sigma_{\hat{Z}}^2. \tag{34}$$

The output signal-to-noise ratio SNR_V has improved linearly with the number of samples integrated J. The input sensitivity improvement through digital integration equals $\sqrt{J}$ for low-input signal-to-noise ratio SNR_i. The dynamic range and threshold sensitivity also increase by the factor $\sqrt{J}$. For example, if the quantization step equals the rms noise ($q = \sigma_{X_n}$) at $J = 1$, then at $J = 4$ there are two quantization levels per noise standard deviation.

The integrating AO channelized receiver provides a direct means for estimating the mean background spectral energy. The background signal may simply be the front end receiver noise as modified by the passband ripple or it may be the average signal environment. If 90-percent confidence is to be obtained that the measurement error in any of say 1000 channels will not exceed one-fourth the standard deviation of the noise in that channel (i.e., [Prob{measurement error $\leqslant \frac{1}{4}$ standard deviation}]^{1000} = 0.9), then the background measurement should be integrated at least 240 times longer than the signal data. The integration settings and detection algorithm are a function of the operational requirement and the spectral environment.

VI. Noise Measurements

The model presented in Section II was substantiated experimentally. Measurements of noise statistics, means and standard deviations, were made on several frequency channel outputs. These measurements were made parametrically on front end receiver noise level and detector integration time. A probability density analyzer was used to record probability densities and cumulative distributions of a frequency channel with signal plus noise input at several signal-to-noise ratios. Measured noise equivalent bandwidths B_s and B_n, agreed with the theory presented in Section III.

The AO channelized receiver had 500 MHz instantaneous bandwidth with 1000 channels spaced at 0.5-MHz intervals. The minimum integration period was 0.25 ms and the detector dynamic range was 33 dB. Analog-to-digital conversion had 10 bits accuracy at a sample rate of 4 MHz.

The front end gain was increased until the noise input to the receiver dominated. The mean noise level was measured for several values of $K = \sigma_{X_n}/\sigma_Y$, and for several integration times. The rms detector noise σ_Y was independent of the detector integration time T. A plot of output noise standard deviation σ_Z versus mean noise level μ_Z is shown in Fig. 6. The ratio μ_Z^2/σ_Z^2 depends linearly on the integration time T. The increase in bias required in order to achieve a constant noise variance is demonstrated. The noise equivalent bandwidth B_n was calculated to be 1.24 MHz for noise input.

Histograms of a single frequency channel output are shown in Fig. 7. The input noise level was set such that $\sigma_{X_n} = 4\,\sigma_Y$. At this setting the maximum sensitivity loss due to detection noise is $\rho = 0.13$ dB. An input CW signal increased the mean output, thereby shifting the probability distribution and increasing the variance. The detector noise only distribution is included for reference. Clearly, the receiver noise dominates.

Equation (11) relating the output variance with sinusoid plus noise to the variance with noise only input can be rewrit-

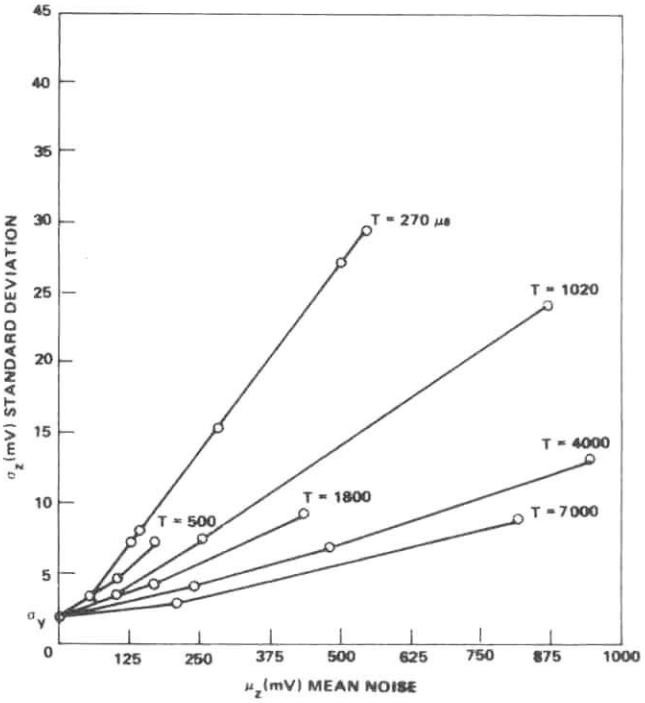

Fig. 6. Standard deviation versus mean noise.

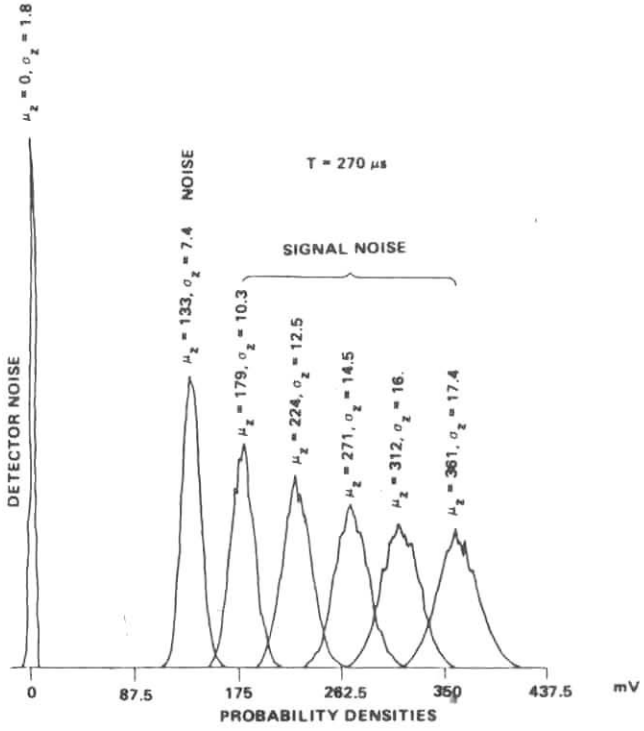

Fig. 7. Probability densities.

ten in terms of measurable quantities μ_s and μ_n as

$$\sigma_{X_{s+n}}^2 = \sigma_{X_n}^2(1 + 2\alpha\mu_s/\mu_n) \tag{35}$$

where

$$\alpha = \sqrt{B_n/B_s}.$$

The noise equivalent bandwidth B_s was calculated by a least squares fit of the measured data to (35). The factor α was

1.38 and the noise equivalent bandwidth was approximately $B_s = 650$ kHz. The experimental value for B_s agrees well with calculations based on a truncated Gaussian window function and trapezoidal spectral weighting model.

The CW input sensitivity can be written as $S = \mathrm{SNR}_Z + kTB_s + NF - \sqrt{B_s T}$. The measured sensitivity was $S = -122$ dBm for 0-dB output signal-to-noise ratio, $T = 0.25$ ms, and $NF = 5$-dB wideband front end noise figure. The measured sensitivity at $JT = 0.256$ s was $S \simeq -137$ dBm ($J = 1024$ samples averaged).

VII. Conclusion

The integrating AO channelized receiver has been applied to the detection of signals buried in noise. A receiver model has been developed and detection statistics were analyzed for sinusoid plus noise and random signal plus noise inputs. Signal-to-noise ratios were defined and noise equivalent bandwidths were derived in terms of input window and spectral weighting functions. The noise equivalent bandwidth was determined to be signal dependent due to spectral averaging. Detection sensitivity and dynamic range were calculated as a function of processing gain and receiver noise loading. Digital processing of channelized receiver data may be used to achieve further sensitivity improvement and increased dynamic range. Linearity and gain stability become increasingly important for large processing gain. Experimental results are in agreement with the statistical model presented. An AO channelized receiver with high sensitivity and wide instantaneous bandwidth has been demonstrated.

Appendix A
Outline for Derivation of Noise Statistics

A.1 Mean Noise Power

The output variable X_{jk} defined by (1) can be rewritten as

$$X_{jk} = \int_{jT}^{(j+1)T} \iiint_{-\infty}^{\infty} H(f - f_k) w(\alpha) w^*(\beta) u(t - \alpha) u(t - \beta) \cdot \exp[-i2\pi f(\alpha - \beta)]\, d\alpha\, d\beta\, df\, dt. \quad (36)$$

For noise only input, i.e., $u(t) = n(t)$, the mean output becomes

$$\mu_n = E\{X_{jk}\} = \int_{jT}^{(j+1)T} \iiint_{-\infty}^{\infty} H(f - f_k) w(\alpha) w^*(\beta) R_n(\alpha - \beta) \cdot \exp[-i2\pi f(\alpha - \beta)]\, d\alpha\, d\beta\, df\, dt. \quad (37)$$

For zero-mean white Gaussian noise with autocorrelation $R_n(\tau) = (N_0/2)\delta(\tau)$ the mean output reduces to

$$\mu_n = \frac{N_0 T}{2} \int_{-\infty}^{\infty} |w(\alpha)|^2\, d\alpha \int_{-\infty}^{\infty} H(f)\, df. \quad (38)$$

Equation (38) is equivalent to (5) through use of Parseval's theorem,

$$\int_{-\infty}^{\infty} G(f)\, df = \int_{-\infty}^{\infty} |w(\alpha)|^2\, d\alpha$$

where $G(f)$ is the magnitude squared of the Fourier transformed window function defined by (6).

A.2 Mean Signal Power

For sinusoid input, $u(t) = A \cos[2\pi f_0 t + \phi]$, the output is (using (36))

$$X_{jk} = \frac{A^2}{2} \int_{jT}^{(j+1)T} \iiint_{-\infty}^{\infty} H(f - f_k) w(\alpha) w^*(\beta) \cdot \{\cos[2\pi f_0(\alpha - \beta)] + \cos[4\pi f_0 t - 2\pi f_0(\alpha + \beta) + 2\phi]\} \cdot \exp[-i2\pi f(\alpha - \beta)]\, d\alpha\, d\beta\, df\, dt. \quad (39)$$

Integrating with respect to t, the output becomes

$$X_{jk} \simeq \frac{A^2 T}{4} \iiint_{-\infty}^{\infty} H(f - f_k) w(\alpha) w^*(\beta) \cdot \{\exp[-i2\pi(f + f_0)(\alpha - \beta)] + \exp[-i2\pi(f - f_0)(\alpha - \beta)]\}\, d\alpha\, d\beta\, df \quad (40)$$

where the term with frequency $2f_0$ has approximately integrated to zero. Integrating $d\alpha d\beta$ and using (6) yields

$$X_{jk} \simeq \frac{A^2 T}{4} \int_{-\infty}^{\infty} H(f - f_k)[G(f + f_0) + G(f - f_0)]\, df \simeq \frac{A^2 T}{4} [\mathcal{H}(f_k - f_0) + \mathcal{H}(f_k + f_0)] \quad (41)$$

where $\mathcal{H}(\cdot)$ is defined by (10). For $f_k \approx f_0$ the term $\mathcal{H}(f_k + f_0)$ is vanishingly small. The mean signal power

$$\mu_s = E\{X_{jk}\} = X_{jk}$$

for deterministic sinusoidal input, resulting in (9).

A.3 Output Variance for Noise Only Input

The variance of the output variable X_{jk} can be calculated as

$$\mathrm{var}\{X_{jk}\} = E\{X_{jk}^2\} - [E\{X_{jk}\}]^2. \quad (42)$$

For noise only input, the mean-square output equals

$$E\{X_{jk}^2\} = \int_{jT}^{(j+1)T} \iint_{jT}^{(j+1)T} \int_{-\infty}^{\infty} \int_{-\infty}^{\infty} \int_{-\infty}^{\infty} \int_{-\infty}^{\infty} \cdot H(f - f_k) H(f' - f_k) w(\alpha) w^*(\alpha') w(\beta) w^*(\beta') \cdot E\{n(t - \alpha) n(t' - \alpha') n(t - \beta) n(t' - \beta')\} \cdot \exp[-i2\pi f(\alpha - \beta)] \exp[-i2\pi f'(\alpha' - \beta')] \cdot d\alpha\, d\alpha'\, d\beta\, d\beta'\, df\, df'\, dt\, dt'. \quad (43)$$

Using the relation for the fourth moment of a jointly Gaussian random process,

$$E\{n(t_1)n(t_2)n(t_3)n(t_4)\} = E\{n(t_1)n(t_2)\} E\{n(t_3)n(t_4)\} + E\{n(t_1)n(t_3)\} E\{n(t_2)n(t_4)\} + E\{n(t_1)n(t_4)\} E\{n(t_2)n(t_3)\}$$

and substituting the noise autocorrelation function, the mean-

square output becomes

$$E\{X_{jk}^2\} = \left(\frac{N_0}{2}\right)^2 \int_{jT}^{(j+1)T} \int_{-\infty}^{\infty} \cdots \int H(f - f_k)H(f' - f_k) \cdot w(\alpha)w^*(\alpha')w(\beta)w^*(\beta') \cdot [\delta(\alpha - \beta)\delta(\alpha' - \beta') + \delta(t - t' + \alpha' - \alpha)\delta(t - t' + \beta' - \beta) + \delta(t - t' + \alpha' - \beta)\delta(t - t' + \beta' - \alpha)] \cdot \exp[-i2\pi f(\alpha - \beta)] \exp[-i2\pi f'(\alpha' - \beta')] \cdot d\alpha\, d\alpha'\, d\beta\, d\beta'\, df\, df'\, dt\, dt'. \quad (44)$$

Integrating the term $\delta(\alpha - \beta)\delta(\alpha' - \beta')$ yields the mean noise power, μ_n^2. Subtracting the mean noise power and using the result

$$\iint_{jT}^{(j+1)T} f(t - t')\, dt\, dt' = T \int_{-T}^{T} (1 - |\tau|/T) f(\tau)\, d\tau \quad (45)$$

the variance can be written as

$$\text{var}\{X_{jk}\} = \left(\frac{N_0}{2}\right)^2 T \int_{-T}^{T} \int_{-\infty}^{\infty} \cdots \int H(f - f_k)H(f' - f_k) \cdot w(\alpha)w^*(\alpha')w(\beta)w^*(\beta')(1 - |\tau|/T) \cdot [\delta(\tau + \alpha' - \alpha)\delta(\tau + \beta' - \beta) + \delta(\tau + \alpha' - \beta)\delta(\tau + \beta' - \alpha)] \exp[-i2\pi f(\alpha - \beta)] \cdot \exp[-i2\pi f'(\alpha' - \beta')]\, d\alpha\, d\alpha'\, d\beta\, d\beta'\, df\, df'\, d\tau. \quad (46)$$

The term $(1 - |\tau|/T)$ may be approximated by unity for T large with respect to the width of $w(\cdot)$. Define the autocorrelation of the input window function as

$$R_w(\tau) = \int_{-\infty}^{\infty} w(t)w^*(t - \tau)\, dt \quad (47)$$

and the Fourier transform of the spectral weighting function as

$$h(t) = \int_{-\infty}^{\infty} H(f) \exp(-i2\pi ft)\, df. \quad (48)$$

Performing the integration results in

$$\text{var}\{X_{jk}\} \simeq \left(\frac{N_0}{2}\right)^2 T \int_{-\infty}^{\infty} |h(\tau)R_w(\tau)|^2\, d\tau \quad (49)$$

where the autocorrelation function (47) is approximated by a finite time estimate, and the function $\mathcal{H}(\cdot)$ vanishes for large argument. The variance for noise only input described by (49) is equivalent to (12) by Parseval's theorem.

A.4 Output Variance for Sinusoid Plus Noise Input

For the case of sinusoid plus noise input

$$u(t) = s(t) + n(t)$$

where

$$s(t) = A \cos[2\pi f_0 t + \phi]$$

the mean-square output equals

$$E\{X_{jk}^2\} = \iint_{jT}^{(j+1)T} \int_{-\infty}^{\infty} \cdots \int H(f - f_k)H(f' - f_k) \cdot w(\alpha)w^*(\alpha')w(\beta)w^*(\beta') \cdot E\{[s(t - \alpha)s(t - \beta) + n(t - \alpha)n(t - \beta) + s(t - \alpha)n(t - \beta) + s(t - \beta)n(t - \alpha)] \cdot [s(t' - \alpha')s(t' - \beta') + n(t' - \alpha')n(t' - \beta') + s(t' - \alpha')n(t' - \beta') + s(t' - \beta')n(t' - \alpha')]\} \exp[-i2\pi f(\alpha - \beta)] \cdot \exp[-i2\pi f'(\alpha' - \beta')]\, d\alpha\, d\alpha'\, d\beta\, d\beta'\, df\, df'\, dt\, dt'. \quad (50)$$

The expectation $E\{\cdot\}$ is comprised of 16 terms. By inspection 8 terms vanish since the noise has zero mean and has zero third moment. The terms $s(\cdot)s(\cdot)s(\cdot)s(\cdot)$ and $n(\cdot)n(\cdot)n(\cdot)n(\cdot)$ become μ_s^2 and $\mu_n^2 + \sigma_{X_n}^2$, respectively. The terms $s(t - \alpha)s(t - \beta)n(t' - \alpha')n(t' - \beta')$ and $s(t' - \alpha')s(t' - \beta')n(t - \alpha)n(t - \beta)$ are both equal to $\mu_s\mu_n$. The terms $s(t - \alpha)s(t' - \alpha')n(t - \beta)n(t' - \beta')$ and $s(t - \beta)s(t' - \beta')n(t - \alpha)n(t' - \alpha')$ are both equal to $(A^2N_0T/4)\mathcal{H}(f_k - f_0)\mathcal{H}(f_k + f_0)$ which is approximately zero for $f_k \approx f_0$. The final two terms $s(t - \alpha)s(t' - \beta')n(t' - \alpha')n(t - \beta)$ and $s(t' - \alpha')s(t - \beta)n(t - \alpha)n(t' - \beta')$ are both equal to $(A^2N_0T/8)[\mathcal{H}^2(f_k - f_0) + \mathcal{H}^2(f_k + f_0)]$. The term $\mathcal{H}^2(f_k + f_0)$ may be dropped for $f_k \approx f_0$. Combining terms, the mean square output is

$$E\{X_{jk}^2\} \approx \sigma_{X_n}^2 + (\mu_s + \mu_n)^2 + \frac{A^2N_0T}{4}\mathcal{H}^2(f_k - f_0) \quad (51)$$

and the output variance is given by

$$\sigma_{X_{s+n}}^2 \approx \sigma_{X_n}^2 \left[1 + \frac{A^2N_0T}{4\sigma_{X_n}^2}\mathcal{H}^2(f_k - f_0)\right]. \quad (52)$$

The variance can be rewritten as

$$\sigma_{X_{s+n}}^2 \approx \sigma_{X_n}^2 \left[1 + \frac{A^2}{B_sN_0}\right] \quad (53)$$

where the noise equivalent bandwidth B_s is defined by (13) and $f_k = f_0$. The output variance (53) is equivalent to (11) with the input signal-to-noise ratio SNR_i measured in a bandwidth B_s.

Appendix B
Shot Noise Consideration

Shot noise results from the photon statistics of the average optical power and is, therefore, signal dependent. The relative importance of shot versus thermal noise depends on the number of thermal noise electrons. The variance of the shot process equals the average number of electrons. Therefore, the expected variance equals $\mu_s + \mu_n$ (measured in electrons). For noise only input ($\mu_s = 0$), the ratio of detector noise variance σ_Y^2 to receiver noise variance $\sigma_{X_n}^2$ is given by

$$\left(\frac{\sigma_Y}{\sigma_{X_n}}\right)^2 = \frac{\sigma_{\text{shot}}^2 + \sigma_{\text{th}}^2}{\sigma_{X_n}^2} = \frac{\mu_n}{\sigma_{X_n}^2} + \frac{\sigma_{\text{th}}^2}{\sigma_{X_n}^2} = \frac{\sqrt{B_nT}}{\sigma_{X_n}} + \left(\frac{\sigma_{\text{th}}}{\sigma_{X_n}}\right)^2$$

where σ_{shot}^2 and σ_{th}^2 are the shot and thermal noise variances, respectively, and all quantities are measured in electrons.

If the ratio of receiver noise to thermal noise is set equal to K, then

$$\left(\frac{\sigma_Y}{\sigma_{X_n}}\right)^2 = \frac{\sqrt{B_n T}}{K\sigma_{\text{th}}} + \frac{1}{K^2}.$$

For example, using $B_n T = 1000$ and $K = 1$, the shot and thermal components are equal for $\sigma_{\text{th}} = \sqrt{B_n T} \simeq 32$ electrons rms. The shot noise becomes less significant with signal plus noise input since the random contribution of shot noise due to the mean signal power μ_s is less than the increase in output variance due to the signal, see (11).

Acknowledgment

The authors wish to acknowledge Carl Clinger for his assistance with instrumentation and noise measurement.

References

[1] T. M. Turpin, "Spectral analysis using optical processing," this issue, pp. 79–92.
[2] A. D. Whalen, *Detection of Signals in Noise*. New York: Academic Press, 1971.
[3] J. D. Kraus, *Radio Astronomy*. New York: McGraw-Hill, 1966.
[4] A. V. Oppenheim and R. W. Schafer, *Digital Signal Processing*. Englewood Cliffs, NJ: Prentice-Hall, 1975, pp. 413–418.